

# Lightning Overvoltages Including Frequency-Dependent Soil Parameters in the Transmission Line Model

R. Alipio, A. De Conti, A. Miranda, M. T. Correia De Barros

**Abstract**—This paper investigates the impact of incorporating frequency-dependent soil parameters on transmission line models for the simulation of lightning transients on overhead transmission lines. Frequency-dependent soil parameters were considered using an alternative implementation of Marti’s transmission line model. Results indicate that the consideration of frequency-dependent soil parameters on transmission line models can be relevant for the simulation of lightning overvoltages on high-voltage transmission lines if the ground is a poor conductor.

**Keywords:** lightning transients, frequency-dependent soil parameters, line modeling, time-domain simulations.

## I. INTRODUCTION

THERE has been an increasing interest in the simulation of electromagnetic transients considering the variation of the ground resistivity and permittivity with frequency. In particular, much work has been done in the last few years to investigate the impact of such frequency dependence on the lightning performance of electrical systems. Such variation has been considered in the simulation of the lightning response of grounding systems [1], [2], in some cases to determine its influence on the lightning performance of transmission lines [3]. In [4], [5], the effect of frequency-dependent soil parameters is considered on the calculation of lightning-induced voltages on distribution lines due to nearby strokes. In [6], such effect is considered in the simulation of electromagnetic transients on overhead power distribution lines.

Despite the recent interest on the subject, a comprehensive analysis of the impact of incorporating frequency-dependent soil parameters on line models for simulating electromagnetic

transients on high-voltage transmission lines is not available in the literature. Therefore, an attempt is made in this paper to investigate possible inaccuracies associated with assuming constant soil parameters in the simulation of lightning transients on high-voltage transmission lines.

## II. TESTED CASE AND MODELING GUIDELINES

To assess the impact of incorporating frequency-dependent soil parameters on line models used for simulating lightning overvoltages, a typical overhead 138-kV Brazilian transmission line is considered. Fig. 1 shows the tower design, which has one ACSR conductor per phase (LINNET) and one 3/8" EHS shield wire. The coordinates of the line cables (in meters) are indicated in the same figure (values within parenthesis are midspan heights).

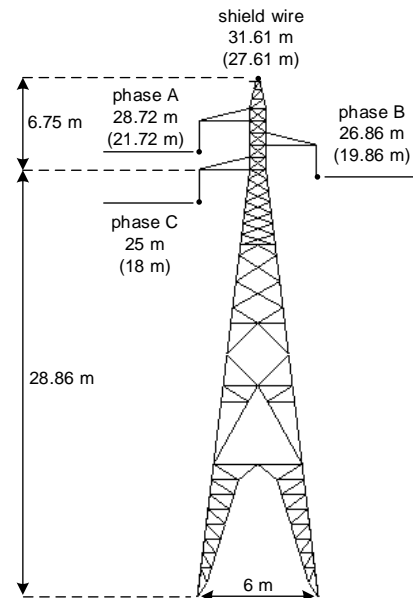


Fig. 1. Tested 138-kV line.

Two strike points are considered in simulations: at the tower top and on the shield wire at the midspan. Two spans of 500 m each are considered at each side of the striking point. To avoid reflections, the line ends are perfectly matched in the whole frequency range using infinitely long lines.

The grounding system of the tower is illustrated in Fig. 2. It consists of four counterpoise wires of 7-mm radius with burial depth of 0.5 m. The total length  $L$  of the counterpoise wires is selected according to the value of low-frequency soil resistivity  $\rho_0$ , as indicated in Table I.

---

This work was supported in part by Brazilian agencies FAPEMIG (grants TEC-APQ-02017-16 and TEC-PPM-00280-17) and CNPq (grant 304117/2016-1).

R. Alipio is with the Department of Electrical Engineering of Federal Center of Technological Education (CEFET-MG), Belo Horizonte, MG, Brazil (e-mail of corresponding author: [rafael.alipio@cefetmg.br](mailto:rafael.alipio@cefetmg.br)).

A. De Conti is with the Federal University of Minas Gerais (UFMG), Belo Horizonte, MG, Brazil (e-mail: [conti@cpdee.ufmg.br](mailto:conti@cpdee.ufmg.br)).

A. Miranda is a graduate student of Electrical Engineering Graduate Program of CEFET-MG, Belo Horizonte, MG, Brazil (e-mail: [audinesena@gmail.com](mailto:audinesena@gmail.com)).

M. T. Correia De Barros is with Instituto Superior Técnico (IST) of University of Lisbon (UL), Lisbon, Portugal (e-mail: [teresa.correiaedebarrros@tecnico.ulisboa.pt](mailto:teresa.correiaedebarrros@tecnico.ulisboa.pt)).

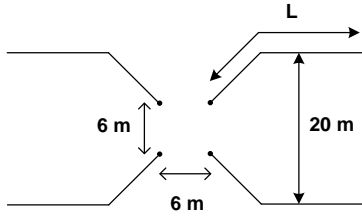


Fig. 2. Typical arrangement of tower-footing grounding electrodes.

TABLE I  
LENGTH OF THE COUNTERPOISE WIRES AS A FUNCTION OF SOIL RESISTIVITY

$\rho_0$ ( $\Omega\text{m}$ )	300	1000	3000
$L$ (m)	20	40	60

### A. Frequency Dependence of Electrical Parameters of Ground

According to measurements performed in laboratory and described in classical papers (e.g., [7]) and to recent experimental results obtained in field conditions (e.g., [8]), the ground conductivity  $\sigma_g$  and permittivity  $\epsilon_g$  are not constant values, but show a strong frequency dependence along the typical frequency range of lightning currents (0 Hz to few MHz). The soil permeability, in general, can be assumed constant and equal to the vacuum permeability,  $\mu_0$  [9].

Recently, equations (1) and (2) were proposed to compute the frequency dependence of ground conductivity  $\sigma_g$  and permittivity  $\epsilon_g$  based on a large number of field measurements and on the causal Kramers-Kronig's relations and Maxwell Equations [8].

$$\sigma_g = \sigma_0 + \sigma_0 \times h(\sigma_0) \left( \frac{f}{1 \text{ MHz}} \right)^\zeta \quad (1)$$

$$\epsilon_g = \epsilon'_\infty + \frac{\tan(\pi\zeta/2) \times 10^{-3}}{2\pi(1\text{MHz})^\zeta} \sigma_0 \times h(\sigma_0) f^{\zeta-1} \quad (2)$$

In (1) and (2),  $\sigma_g$  is the ground conductivity in mS/m,  $\sigma_0=1/\rho_0$  is the DC conductivity in mS/m,  $\epsilon_g$  is the ground permittivity in F/m,  $\epsilon'_\infty$  is the ground permittivity at higher frequencies and  $f$  is the frequency in Hz. According to [8], the following parameters are recommended in (1) and (2) to obtain mean results for the frequency variation of  $\sigma_g$  and  $\epsilon_g$ :  $\zeta = 0.54$ ,  $\epsilon'_\infty = 12\epsilon_0$  and  $h(\sigma_0) = 1.26 \times \sigma_0^{-0.73}$ , where  $\epsilon_0$  is the vacuum permittivity.

### B. Transmission Line Model

Two models are adopted in this paper to represent the high-voltage transmission line. One of them is the line model proposed by Marti [10], which is possibly the most popular model for the digital simulation of electromagnetic transients on overhead lines. Briefly, it is a distributed-parameter model that includes the variation of the line parameters with frequency. The solution of the transmission line equations is performed in the modal domain, considering a constant and real transformation matrix. The JMarti setup available in the LCC routine of ATPDraw considers Carson's equations for calculating the parameters of overhead transmission lines [11]. Among other aspects, Carson's equations assume that  $\sigma_g \gg \omega\epsilon_g$ , i.e., displacement currents in the soil are negligible

in comparison with conductive currents. Furthermore, the frequency dependence of soil parameters is disregarded.

In order to evaluate the effect of frequency-dependent soil parameters in the simulation of lightning overvoltages on overhead transmission lines, an alternative implementation of Marti's model, herein called "modified Marti's model", is used. This implementation, which was proposed in [6], consists in calculating the ground-return impedance with Sunde's formulation [12] [expressed by (3), (4) and (5) below] assuming the soil parameters to vary as described in (1) and (2). The vector fitting technique [13] is used for fitting the characteristic impedance and the propagation function of each transmission line mode using a dedicated set of poles and residues. The real transformation matrix necessary for the time domain simulations is calculated at a selected frequency. Finally, the obtained poles and residues are written, together with the minimum time delays of each mode and the real transformation matrix, in the form of a .pch file that is interpreted in ATP as a transmission line model of Marti type (see [6] for details).

Considering Sunde's equations, the self and mutual terms of the ground-return impedance matrix of a multiphase overhead transmission line can be calculated with [12]

$$Z_{g'ii} = \frac{j\omega\mu_0}{\pi} \int_0^\infty \frac{e^{-2h_i\lambda}}{\sqrt{\lambda^2 + \gamma_g + \lambda}} d\lambda \quad (3)$$

$$Z_{g'ij} = \frac{j\omega\mu_0}{\pi} \int_0^\infty \frac{e^{-(h_i+h_j)\lambda}}{\sqrt{\lambda^2 + \gamma_g + \lambda}} \cos(r_{ij}\lambda) d\lambda \quad (4)$$

where

$$\gamma_g = \sqrt{j\omega\mu_0(\sigma_g + j\omega\epsilon_g)} \quad (5)$$

in which  $\mu_0=4\pi \times 10^{-7}$  H/m,  $\epsilon_0 \approx 8.854 \times 10^{-12}$  F/m,  $\omega$  is the angular frequency, in rad/s,  $r_{ij}$  is the horizontal separation between conductors  $i$  and  $j$ , in m,  $h_i$  and  $h_j$  are the heights of conductors  $i$  and  $j$ , in m.

### C. Tower

The tower is modeled as a lossless single-phase line. The surge impedance of this line is calculated with the revised Jordan's formula, which was extended in [14] to take into account vertical multiconductor systems. Considering that the tower can be represented by  $n$  vertical conductors and that they are connected at the current injection point, it is possible to represent the whole multiconductor system as a single transmission line with equivalent surge impedance  $Z_{eq}$  given by [14]

$$Z_{eq} = \frac{V}{I} = \frac{Z + Z_{12} + Z_{13} + \dots + Z_{1n}}{n} \quad (6)$$

where

$$Z = 60 \left[ \ln \frac{4h}{r} - 1 \right] \quad (7)$$

$$Z_{ij} = 60 \ln \frac{2h + \sqrt{4h^2 + d_{ij}^2}}{d_{ij}^2} + 30 \frac{d_{ij}}{h} - 60 \sqrt{1 + \frac{d_{ij}^2}{4h^2}} \quad (8)$$

In (7) and (8),  $h$  is the height of the conductor,  $r$  is the conductor radius, and  $d_{ij}$  corresponds to the distance between the centers of conductors  $i$  and  $j$ . In particular, the tower of Fig. 1 was divided into four sections, each one represented by four vertical conductors. The lower portion of the tower was represented as a cascade of three transmission lines (two 9-m long and one 8.86-m long), while its upper part was represented as a single 6.75-m long transmission line. This was made to consider the variation of the cross section of the tower with position, which changes the mutual surge impedance as a function of height. The equivalent impedance of each tower segment was computed using (6), (7) and (8), considering average distances between tower conductors and assuming  $r=6.5$  cm. The tower model is shown in Fig. 3.

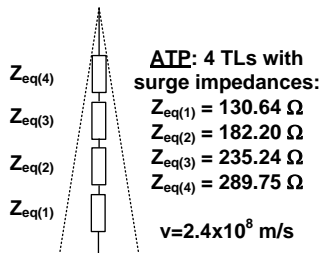


Fig. 3. Tower model.

#### D. Tower-footing Grounding

The tower-footing grounding system plays a fundamental role in backflashover occurrence when the shield wire and the tower are subjected to direct strikes. Recently, it was shown that the frequency dependence of soil parameters significantly affects the lightning response of grounding electrodes [1]. Therefore, it is important to include this feature in ATP simulations to accurately determine resultant lightning overvoltages along the line. The methodology used to simulate the frequency-dependent behavior of tower-footing grounding in ATP is briefly described below.

First, the harmonic impedance  $Z(j\omega)$  of the tower-footing grounding is determined using the accurate Hybrid Electromagnetic Model (HEM) [15], in a frequency range from dc to several megahertz. In the calculations, the frequency dependence of the soil parameters is taken into account using (1) and (2). After determining the harmonic impedance  $Z(j\omega)$ , a pole-residue model of the associated admittance  $Y(j\omega)=1/Z(j\omega)$  is obtained using the vector fitting technique [12]. Finally, an electrical network that is suitable to time-domain simulations is determined from the passive pole-residue model corresponding to the grounding admittance. Both the pole-residue model and the electrical network were obtained using the vector fitting technique [16].

#### E. Lightning Current

According to measurements performed in instrumented towers, first stroke currents of downward negative lightning are characterized by a pronounced concavity at the front and by the occurrence of multiple peaks. Generally, the second peak presents the highest current amplitude, whereas the maximum steepness occurs near the first peak [17]. Considering these aspects, the current waveform illustrated in

Fig. 4, which closely reproduces the median parameters of first strokes measured at Mount San Salvatore [18], is used in the simulations. As discussed in [17], the waveform of Fig. 4 is represented as the sum of seven Heidler functions.

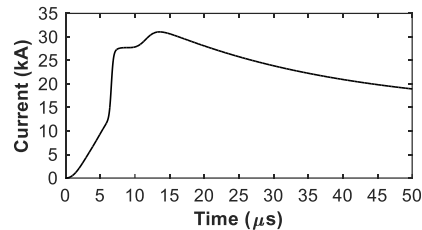


Fig. 4. Representative lightning current waveform of first strokes measured at Mount San Salvatore.

### III. RESULTS

This section presents simulation results of lightning transients on the overhead line illustrated in Fig. 1 incorporating the effect of frequency-dependent ground conductivity and permittivity in the calculation of the transmission line parameters. The following sections discuss different aspects of the performed simulations. First, in Section III-A, with the aim of shading some light on the basic aspects of the influence of incorporating frequency-dependent soil parameters on the line model, a single section of the line is considered. Then, sections III-B and -C present results of the simulated lightning overvoltages on the transmission line considering, respectively, the strike point at the tower top and at the midspan.

#### A. Analysis of a Single Line Span

To illustrate the influence of frequency-dependent soil parameters on the propagation of lightning overvoltages, a simulation with a 500-m long line was performed neglecting the presence of the tower and of the tower-footing grounding. The lightning current of Fig. 4 was injected by an ideal current source at the sending ending of the shield wire. A lumped resistance of  $100 \Omega$  was connected at the receiving end of the shield wire, while all other terminals remained open. Figs. 5-7 illustrate the voltages calculated at the receiving end of the shield wire and at the lower phase. Three values of low-frequency soil resistivity  $\rho_0=1/\sigma_0$  were considered, namely 300, 1000 and 3000  $\Omega\text{m}$ .

According to the results, no noticeable differences are observed in the calculated voltages at the receiving end of the shield wire, regardless of the value of low-frequency soil resistivity. On the other hand, the induced voltages at the receiving end of the lower phase present a distinct behavior, both in terms of amplitude and waveform, depending on the line model. The inclusion of frequency-dependent soil parameters, considered in the modified Marti's model, leads to an increase in damping and waveform distortion compared to the classical Marti's model, which assumes constant soil parameters. The differences observed in the voltage waveforms calculated assuming or neglecting the variation of the soil parameters with frequency become more pronounced with increasing low-frequency soil resistivity.

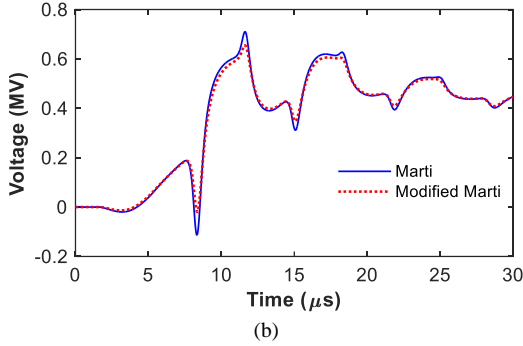
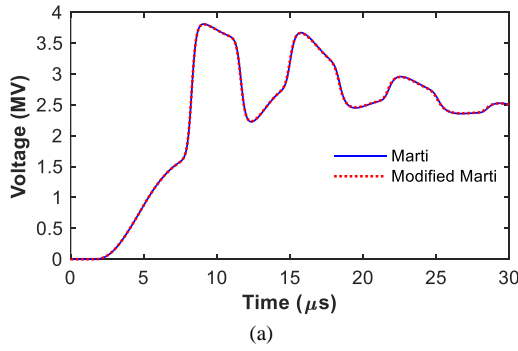


Fig. 5. Voltages at the receiving end of the line in response to the injection of the lightning current of Fig. 4, considering (modified Marti's model) and neglecting (Marti's model) the frequency variation of soil parameters for a resistivity  $\rho_0=300 \Omega\text{m}$ . Phase terminals open. (a) Receiving end of shield wire, (b) receiving end of lower phase.

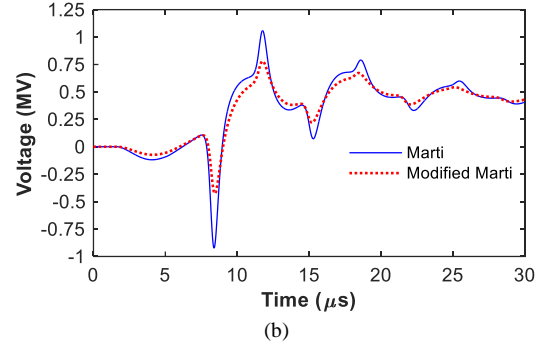
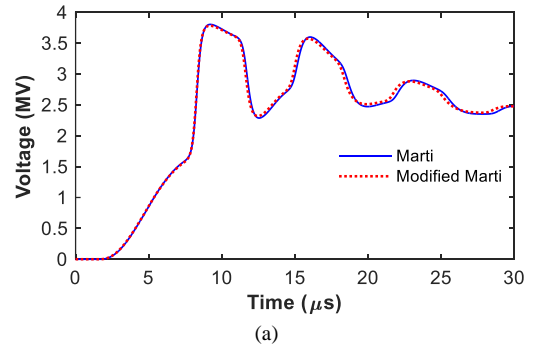


Fig. 7. Same as Fig. 5, but for a soil resistivity  $\rho_0=3000 \Omega\text{m}$ .

### B. Strike Point at Tower Top

In this section, lightning overvoltages calculated in the complete system considering the tower and the tower-footing grounding are presented for the strike point at the tower top. The lightning current is now injected through a Norton-type current source with internal resistance of  $1500 \Omega$ , which represents the lightning channel impedance as seen from the injection point [19]. Fig. 8(a) and Fig. 8(b) illustrate the calculated voltages at the top of the tower and at the lower phase conductor, respectively. Fig. 8(c) illustrates the difference between these two voltages, which is equivalent to the voltage across the insulator string if a pure TEM-field structure is assumed.

When the lightning stroke hits the tower top, the lightning current and the associated voltage wave split into three components: two of them travel through the shield wires toward the adjacent towers and a third component travels downward the struck tower. When reaching the bottom of the tower, part of this last component is transmitted to the grounding system and part of it is reflected back to the tower top. As a consequence, the voltage at the tower top is mainly determined by the superposition of the incident downward wave and the reflected wave at the bottom of the tower. The incident and reflected waves are determined, respectively, by the tower surge impedance and the tower footing grounding impedance. This explains why the tower top voltage illustrated in Fig. 8(a) is basically insensitive to the line model. Considering typical span lengths, reflections coming from adjacent towers will have an influence on the voltage at the tower top only after its peak value. Anyway, considering the results of Fig. 8(a), even along the wavetail, the voltage curves are nearly insensitive to the line model.

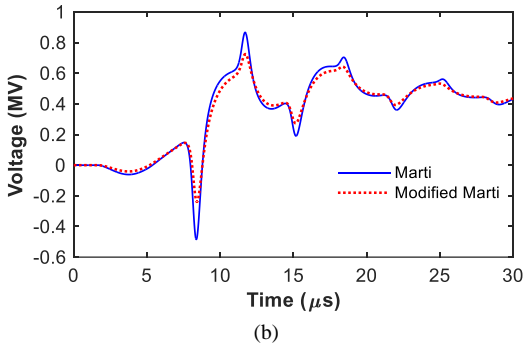
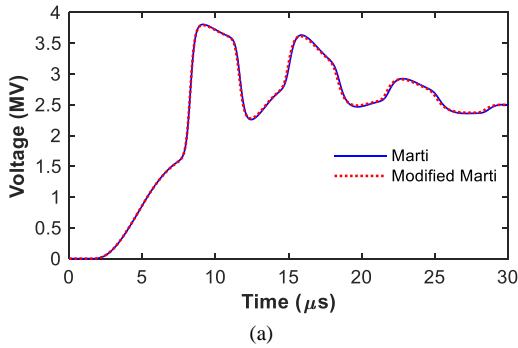


Fig. 6. Same as Fig. 5, but for a soil resistivity  $\rho_0=1000 \Omega\text{m}$ .

As discussed above, the difference between results obtained considering both line models is more significant in the case of a poorly-conducting ground. Thus, results presented in the next sections are focused on the soil resistivity of  $3000 \Omega\text{m}$ .

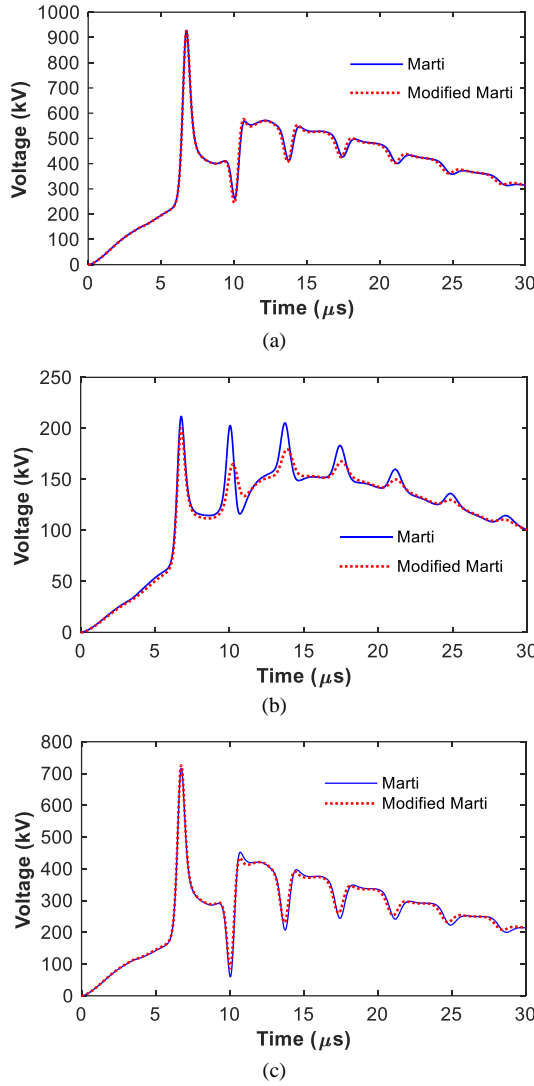


Fig. 8. Voltages (a) at the top of the tower, (b) at the lower phase, and (c) across the lower insulator string for current injection to the tower top, considering (modified Marti's model) or neglecting (Marti's model) the frequency variation of soil parameters for a soil resistivity  $\rho_0=3000 \Omega\text{m}$ .

In Fig. 8(b), which illustrates the voltage at the lower phase conductor, more noticeable differences are observed in the curves calculated considering or neglecting the variation of the soil parameters with frequency. In particular, the peak value of the induced voltage is 6% lower when frequency-dependent soil parameters are assumed. Along the wave tail, the observed differences are more significant. This is due to the effect of ground losses on the traveling waves along the shield wire, which becomes more pronounced as a consequence of multiple reflections and also affects the voltage induced on the phase conductors.

In practice, the voltage across the insulator string is the most important parameter for assessing the lightning performance of a transmission line. As mentioned before, it corresponds approximately to the difference between the voltage wave at the top of the tower and the induced voltages at the phase conductors. Fig. 8(c) shows that the voltage across the lower insulator string is nearly model independent at the wavefront. This can be explained as follows: in

determining the voltage across line insulator, the voltage at the tower top is dominant, since it is about four times larger than the induced voltage at phase conductor. Since the assumed line model does not have any influence on the early time behavior of the tower top voltage, no significant differences are observed along the front of the voltages calculated across the insulator using both line models. Considering the analyzed case, the peak value of the voltage across the insulator string is only about 2% higher when frequency-dependent soil parameters are assumed. Along the wave tail, differences between the waveforms are more noticeable; however, such differences are likely to play a minor role in the determination of the occurrence (or not) of insulator string flashover.

### C. Strike Point at Midspan

In this section, lightning overvoltages calculated in the complete system considering the tower and the tower-footing grounding are presented for the strike point at the midspan. The same conditions assumed in the previous section are considered. The midspan voltages are shown in Fig. 10(a), for the shield wire, and Fig. 10(b), for the higher phase conductor. Although such voltages are expected to be affected by corona, this effect was neglected to keep the analysis focused on the influence of frequency-dependent soil parameters on the resulting overvoltages.

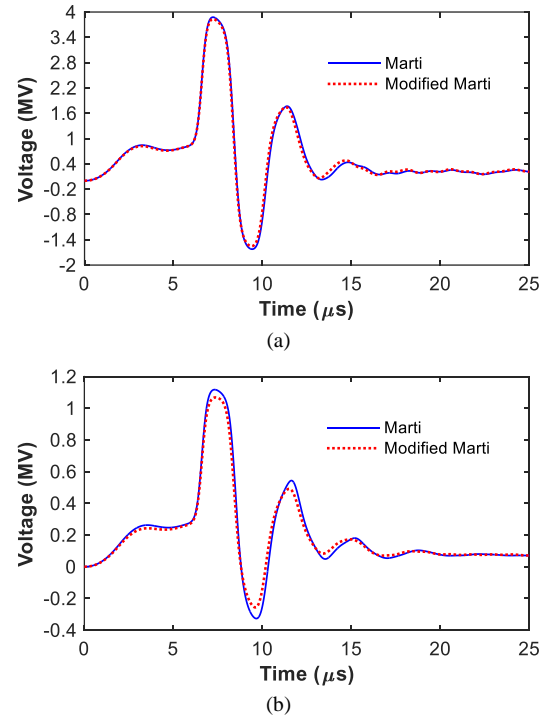


Fig. 10. Midspan voltages on (a) shield wire and (b) higher phase conductor considering (modified Marti's model) or neglecting (Marti's model) the frequency variation of soil parameters for a soil resistivity  $\rho_0=3000 \Omega\text{m}$  and current injection into the shield wire at the midspan.

It is seen in Fig. 10(a) that the shield wire voltage is nearly independent on the assumed line model. Although the voltage at the upper phase conductor, shown Fig. 10(b), is subjected to higher damping due to the frequency variation of the soil parameters, the effect of such variation is minimal. In any

case, since the voltage between the shield wire and the upper phase is mainly dependent on the former, it can be said that the consideration of the frequency variation of soil parameters probably does not affect the occurrence of an eventual flashover at the midspan.

Fig. 11 illustrates the voltage waveform across the lower insulator string of the first tower on the left of the strike point. The differences between overvoltages calculated considering or neglecting the frequency variation of soil parameters are perceptible in this case. The mechanism of overvoltage development at the insulator string can be explained using the same concepts of the previous section. However, in the case of midspan incidence, before traveling downward the structure toward the grounding system, the voltage wave travels along the shield wire. Then, the resultant voltage waveform across the line insulators is different, in comparison to a direct incidence to the top of the tower. In particular, it is seen that the voltage presents an oscillatory behavior. The inclusion of the variation of the soil parameters with frequency leads to higher damping of the oscillatory voltage. Considering Fig. 11, the first three peaks of the voltage wave are 8%, 42% and 11% lower when the frequency variation of soil parameters is incorporated in the line model. It should be mentioned that the differences observed in the calculated voltages, considering or neglecting the frequency dependence of soil parameters, could be determinant for the occurrence or not of insulator string flashover.

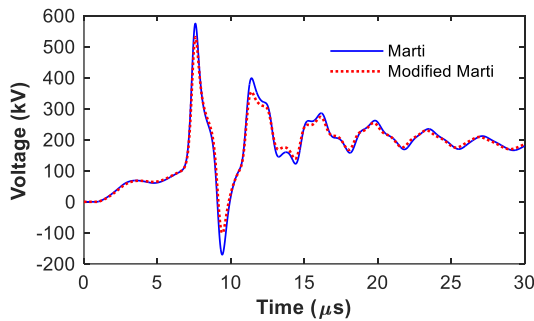


Fig. 11. Voltage across the lower insulator string of the first tower on the left of the strike point, for a current injection to the shield wire at midspan, considering (modified Marti's model) or neglecting (Marti's model) the frequency variation of soil parameters for a soil resistivity  $\rho_0=3000 \Omega\text{m}$ .

#### IV. CONCLUSIONS

This paper investigates the influence of considering frequency-dependent soil parameters in the calculation of transmission line parameters in the assessment of lightning overvoltages on high-voltage transmission lines. Results show relevant differences in simulated lightning overvoltages assuming or neglecting the frequency dependence of soil parameters, notably considering the strike point at the midspan. These differences became more pronounced with increasing the value of the soil resistivity and might be important in determining the line backflashover. Overall, if accurate estimates of the lightning performance of a transmission line are required, the frequency dependence of soil parameters should be incorporated on transmission line models, especially if the ground is a poor conductor.

It is worth mentioning that the results presented in this paper correspond to voltages due to the injection of a median lightning current waveform. Considering the statistical nature of lightning, currents with a shorter front time than the one considered in the analysis can also strike the line. In this case, due to the higher frequency content of the current, the differences observed between the voltage waveforms calculated assuming or neglecting the variation of the soil parameters with frequency may be more pronounced.

#### V. REFERENCES

- [1] R. Alipio and S. Visacro, "Frequency dependence of soil parameters: effect on the lightning response of grounding electrodes," *IEEE Trans. Electromagnetic Compatibility*, vol. 55, no. 1, pp. 132–139, Feb. 2013.
- [2] M. Akbari, K. Sheshyekani, and M. R. Alemi, "The effect of frequency dependence of soil electrical parameters on the lightning performance of grounding systems," *IEEE Trans. Electromagnetic Compatibility*, vol. 55, no. 4, pp. 739–746, Aug. 2013.
- [3] S. Visacro and F. Silveira, "The impact of the frequency dependence of soil parameters on the lightning performance of transmission lines," *IEEE Trans. Electromagnetic Compatibility*, vol. 57, no. 3, pp. 434–441, Jun. 2015.
- [4] M. Akbari, K. Sheshyekani, A. Pirayesh, F. Rachidi, M. Paolone, A. Borghetti, and C. A. Nucci, "Evaluation of lightning electromagnetic fields and their induced voltages on overhead lines considering the frequency dependence of soil electrical parameters," *IEEE Trans. Electromagnetic Compatibility*, vol. 55, no. 5, pp. 1210–1219, Dec. 2013.
- [5] F. H. Silveira, S. Visacro, R. Alipio, and A. De Conti, "Lightning-induced voltages over lossy ground: the effect of frequency dependence of electrical parameters of soil," *IEEE Trans. Electromagnetic Compatibility*, vol. 56, no. 5, pp. 1129–1136, Oct. 2014.
- [6] A. De Conti and M. P. S. Emídio, "Extension of a modal-domain transmission line to include frequency-dependent ground parameters," *Electric Power System Research*, vol. 138, pp. 120–130, 2016.
- [7] J. H. Scott, "Electrical and magnetic properties of rock and soil," U.S. Geol. Surv., Dep. of the Interior, Washington, D.C., 1966.
- [8] R. Alipio and S. Visacro, "Modeling the frequency dependence of electrical parameters of soil," *IEEE Trans. Electromagn. Compat.*, vol. 56, no. 5, pp. 1163–1171, Oct. 2014.
- [9] C. M. Portela, "Measurement and modeling of soil electromagnetic behavior," in Proc. IEEE Int. Sym. Electromagnetic Compatibility, Seattle, WA, 1999, pp. 1004–1009.
- [10] J. R. Marti, "Accurate modelling of frequency-dependent transmission lines in electromagnetic transient simulation," *IEEE Transactions on Power Apparatus and Systems*, vol. PAS-101, no. 1, pp. 147–157, Jan. 1982.
- [11] L. Prikler, H.K. Hoidalen, ATPDraw Manual, Version 5.6, 2009.
- [12] E. D. Sunde, Earth Conduction Effects in Transmission Systems, Dover Publications, New York, 1968.
- [13] B. Gustavsen and A. Semlyen, "Rational approximation of frequency domain responses by vector fitting," *IEEE Trans. Power Delivery*, vol. 14, pp. 1052–1061, July 1999.
- [14] A. De Conti, S. Visacro, A. Soares, and M. A. O. Schroeder, "Revision, extension and validation of Jordan's formula to calculate the surge impedance of vertical conductors," *IEEE Trans. Electromagn. Compat.*, vol. 48, n. 3, pp. 530–536, Aug. 2006.
- [15] S. Visacro and A. Soares Jr., "HEM: a model for simulation of lightning-related engineering problems," *IEEE Trans. Power Delivery*, vol. 20, no. 2, pp. 1026–1208, Apr. 2005.
- [16] B. Gustavsen, Matrix Fitting Toolbox [Online]. Available: <https://www.sintef.no/projectweb/vectfit/>, 2009.
- [17] A. De Conti and S. Visacro, "Analytical representation of single- and double-peaked lightning current waveforms," *IEEE Trans. Electromagnetic Compatibility*, vol. 49, no. 2, pp. 448–451, May 2007.
- [18] K. Berger, R. B. Anderson, and H. Kroninger, "Parameters of lightning flashes," *Electra*, no. 80, pp. 223–237, 1975.
- [19] V. Rakov, "Transient response of a tall object to lightning," *IEEE Trans. Electromagnetic Compatibility*, vol. 43, no. 4, pp. 654–661, Nov. 2001.